Miller cycle combined with EGR and post fuel injection for emissions and exhaust gas temperature control of a heavy-duty diesel engine

Wei Guan[1], Vinícius B. Pedrozo[1], Hua Zhao[1], Zhibo Ban[2], Tiejian Lin[2]

([1]Brunel University London, UK; [2]Guangxi Yuchai Machinery Company, China)

Abstract

Miller cycle has been shown as a promising engine strategy to reduce in-cylinder nitrogen oxides (NOx) formation during the combustion process and facilitate its removal in the aftertreatment systems (ATS) by increasing the exhaust gas temperature (EGT). However, the level of NOx reduction and the increase in EGT achieved by Miller cycle alone is limited. Therefore, research was carried out to investigate the combined use of Miller cycle with other advanced combustion control strategies in order to minimise the NOx emissions and the total cost of ownership.

In this paper, the effects of Miller cycle, exhaust gas recirculation (EGR), and post injection were studied and analysed on the performance and exhaust emissions of a single cylinder heavy-duty (HD) diesel engine. A cost-benefit analysis was carried out using the corrected total fluid efficiency, which includes the estimated urea solution consumption in the NOx aftertreatment system as well as the fuel consumption. The experiments were performed at a low load of 6 bar net indicated mean effective pressure (IMEP). The results showed that the application of a Miller cycle-only strategy with a retarded IVC at -95 CAD ATDC decreased NOx emissions by 21% to 6.0 g/kWh and increased EGT by 30% to 633K when compared to the baseline engine operation. This was attributed to a reduction in compressed gas temperature by the lower effective compression ratio (ECR) and the in-cylinder mass trapped due to the retarded IVC. These improvements, however, were accompanied by a fuel efficiency penalty of 1%. A further reduction in the level of NOx from 6.0 to 3.0 g/kWh was achieved through the addition of EGR, but soot emissions were more than doubled to 0.022 g/kWh. The introduction of a post injection was found to counteract this effect, resulting in simultaneous low NOx and soot emissions of 2.5 g/kWh and 0.012 g/kWh, respectively. When taking into account the urea consumption, the combined use of Miller cycle, EGR and post injection combustion control strategies were found to have relatively higher corrected total fluid efficiency than the baseline case. Thus, the combined “Miller cycle + EGR + post injection” strategy was the most effective means of achieving simultaneous low exhaust emissions, high EGT, and increased corrected total fluid efficiency.

Keywords

Heavy-duty diesel engine, Miller cycle, EGR, post injection, exhaust gas temperatures

1. Introduction

HD diesel engines are widely used in the commercial vehicle sector due to their high torque output, reliability, and durability, as well as their superior thermal efficiency. However, conventional diesel engines can produce significant pollutants, particularly NOx and soot emissions. This is due to the existence of locally fuel-rich and high combustion temperature zones resulted from the non-premixed diffusion-controlled combustion [1]. Ever-stringent emissions and fuel efficiency regulations coupled with the customers requirement to reduce the vehicle operational cost, have pushed engine manufacturers to pursue highly efficient and ultra-clean combustion technologies for internal combustion engines [2].

Low temperature combustion (LTC) concepts such as Homogeneous Charge Compression Ignition (HCCI), Premixed Charge Compression Ignition (PCCI), and Partially Premixed Charge Compression Ignition (PPCI) have been developed to produce low engine-out emissions. These are generally centred on enhancing the quality of fuel-air mixing and increasing the degree of pre-mixed combustion, and therefore reduced the locally fuel-rich regions and peak in-cylinder gas temperature [3–5]. As a result, a simultaneous reduction in NOx and soot emissions can be obtained, but these LTC modes tend to suffer from higher unburnt hydrocarbons (HC) and carbon monoxide (CO) emissions [6,7]. Additionally, the aggressive use of EGR and the corresponding high boost pressure requirements limited the engine operating range.

In addition to the high levels of NOx and soot formation in the conventional diesel combustion, relatively lower EGT at low engine operation loads limits the efficient conversion of exhaust pollutants in the ATS. The conversion efficiencies of ATS used in diesel engines such as selective catalytic reduction (SCR), diesel particulate filter (DPF), and diesel oxidation catalyst

(DOC) are highly dependent on the EGT [8–10]. Thus, it is essential to develop effective in-cylinder combustion control strategies to manage the EGT as well as the engine-out emissions, decreasing the engine operational cost.

Miller cycle, achieved by early or late intake valve closing (IVC) timings, has been adopted in gasoline engines for reduced pumping loss at low load and suppression of knocking combustion and NOx reduction at high load operations [11–13]. However, the practical application of the Miller cycle to diesel engines is more challenge. This is mainly due to the limited operation range and relatively smaller benefit achieved when compared to gasoline engines [14], as diesel engines have lower throttling loss and a better scavenging performance. In addition, the Miller cycle would also reduce the volumetric efficiency due to the lower charging efficiency caused by LIVC timing [15,16]. Furthermore, a variable valvetrain and the higher performance turbocharging system to maintain power density would increase the engine's cost [11]. Previously, the main interest of applying Miller cycle in diesel engines is for emissions control in marine applications by lowering the in-cylinder gas temperatures at the end of the compression stroke [17–19]. In recent years, however, the main research focus have been on the reduction of NOx emissions from on-road diesel vehicles as the emissions regulation become increasingly stringent [20–24].

Wang et al. [25] experimentally investigated the application of Miller cycle in a diesel engine for NOx emissions control, decreasing NOx emissions by up to 17.5%. Experimental and numerical studies by Rinaldini et al. [14] showed the Miller cycle strategy could led to simultaneous reduction in NOx and soot emissions by 25% and 60% respectively, but with a fuel efficiency penalty of 2% in a light-duty diesel vehicle in the European Driving Cycle. The NOx reduction obtained by Miller cycle was a result of the lower charging efficiency and combustion temperatures [26]. Studies also showed that the Miller cycle combined with higher intake pressure can effectively minimize NOx emissions while increasing the engine performance [27,28].

Other works have also show that Miller cycle can be an effective strategy for exhaust gas temperature management [8,29,30]. This is mainly attributed to the lower in-cylinder mass resulted from the delayed IVC timing, leading to a lower in-cylinder heat capacity. The experimental and numerical study by Ratzberger et al. [31] demonstrated the potential of an early exhaust valve opening (EEVO) and a late intake valve closing (LIVC) for exhaust thermal management. Garg et al. [32] experimentally examined the influence of in-cylinder charge control via early and late IVC events at a low engine load. A significant increase in turbine outlet temperatures from 195ºC to 255ºC was achieved by both IVC strategies.

Despite many studies have demonstrated the capability of Miller cycle for NOx emissions control, the level of NOx reduction achieved by Miller cycle alone is limited in diesel engines, particularly at low engine loads [16]. This is primarily due to the relatively small impact on the peak in-cylinder gas temperature at low load operations [26,33]. External EGR, however, is a proven technology for NOx formation control [34], because of their thermal, chemical, and dilution effects [35]. Some studies [36–39] have investigated the combined use of Miller cycle and EGR and have demonstrated that this strategy is effective in minimising engine-out NOx emissions.

Kim et al. [16] investigated the effects of LIVC with EGR on engine performance and emissions of a single cylinder diesel engine operating at low load conditions. The LIVC strategy alone demonstrated a limited NOx emissions reduction. With appropriate combination of LIVC and EGR, a reduction in the NOx emissions from more than 10 g/kWh to less than 1 g/kWh was obtained with slight penalty on the IMEP. Benajes et al. [40] studied the impact of early intake valve closing (EIVC) timing coupled with different intake oxygen concentrations (e.g. EGR rates) at low engine load. According to the analysis, EIVC showed its potential for NOx emissions control due to the lower peak in-cylinder gas temperature.

However, the lower in-cylinder gas temperatures in the burned zone deteriorated the combustion process and slowed down the oxidation of soot and CO emissions, increasing the levels of engine-out soot and CO emissions [40,41]. Although advanced injection timing, higher injection pressure, and higher boost pressure can be used to compensate this drawback, they can reduce EGT and the NOx-soot and NOx-CO trade-offs remain. In addition, these strategies would increase the engine operational cost when considering the total fluid consumption including diesel fuel and the estimated urea consumption in the SCR system.

In order to resolve these issues, a systematic study was carried out to investigate combined use of Mille cycle with advanced in-cylinder combustion control strategies to reduce in-cylinder NOx formation and improve the EGT management while minimising the engine operational cost as well as soot and CO emissions. In particular, the current work is the first attempt to experimentally explore the Miller cycle combined with EGR and post injection for low load emissions and EGT control. Therefore, this work includes a good novelty and originality.

The experiments were conducted on a single cylinder HD diesel engine at an engine speed of 1250 rpm and load of 6 bar IMEP, which represents a high residency area in a typical HD drive cycle and has a relatively higher weighing factor in the World Harmonized Stationary Cycle (WHSC) [42]. A one-dimensional (1D) engine simulation model was used to calculate the mean in-cylinder gas temperatures (T_m) and burned zone gas temperatures (T_b) based on experimental pressure measurements. The effectiveness of Miller cycle was defined and evaluated, followed by the analysis of a Miller cycle engine operation combined with EGR and post injection. Finally, a cost-benefit and overall emissions analysis of all advanced combustion control strategies were examined and compared to the baseline case.

2. Experimental setup

2.1 Overview

Figure 1 shows the schematic of the experimental setup, which consists of a single cylinder HD diesel engine equipped with a high pressure common rail fuel injection system, an eddy current dynamometer, an external boosting device, as well as measurement equipment and a data acquisition system (DAQ). The key specifications of the engine are listed in Table 1. The design of cylinder head with 4-valve and a stepped-lip piston bowl were based on the Yuchai YC6K six-cylinder engine, while the bottom end/short block was AVL-designed with two counter-rotating balance shafts.

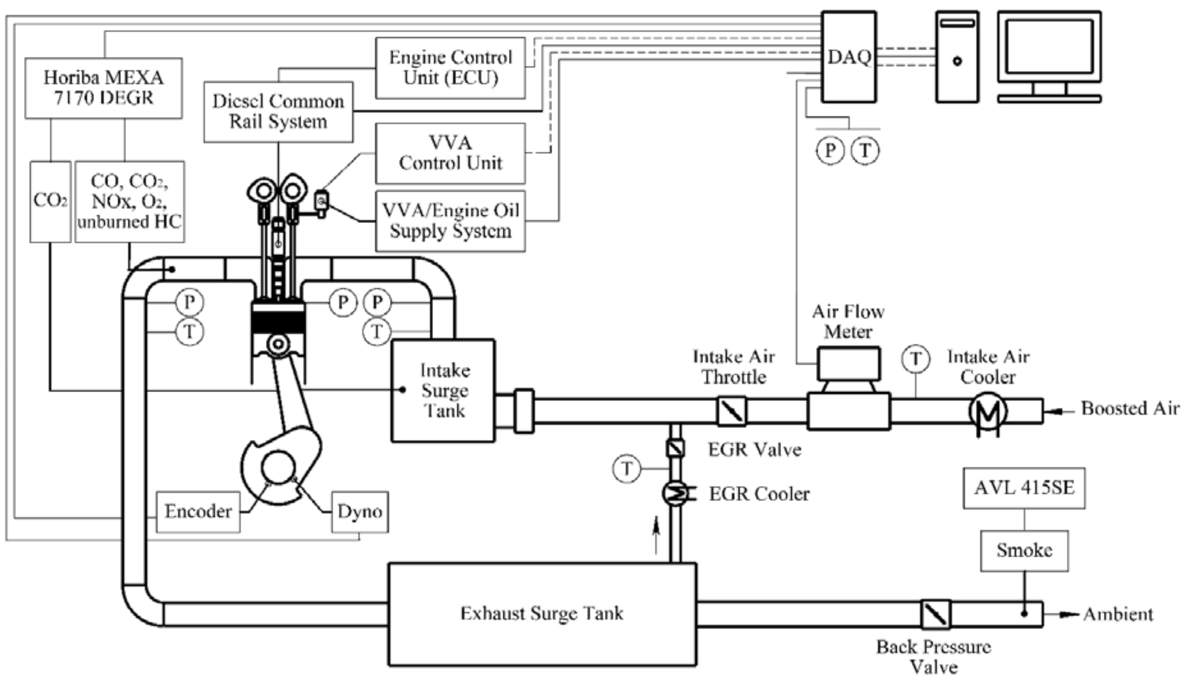

Figure 1. Layout of the engine experimental setup.

Table 1. Specifications of the test engine.

Displaced Volume	2026 cm^3
Stroke	155 mm
Bore	129 mm
Connecting Rod Length	256 mm
Geometric Compression Ratio	16.8
Number of Valves	4
Piston Type	Stepped-lip bowl
Diesel Injection System	Bosch common rail
Nozzle design	8 holes, included spray angle of 150°
Maximum fuel injection pressure	2200 bar
Maximum in-cylinder pressure	180 bar

2.2 Variable valve actuation system

The engine was equipped with a lost motion variable valve actuation (VVA) system, which incorporated a hydraulic tappet on the valve side of the rocker arm. This system allowed for Miller cycle operation via LIVC. The intake valve opening (IVO) and IVC timings of the baseline case were set at 367 and -174 crank angle degrees (CAD) after top dead centre (ATDC) respectively. The maximum intake valve lift event was 14mm. Figure 2 shows the intake and exhaust valve profiles for the baseline and Miller cycle operations. All valve events in this study were considered at 1 mm valve lift. The effective compression ratio (ECR) was calculated as

$$ECR = \frac{V_{ivc\_eff}}{V_{tdc}} \quad (1)$$

where V_{tdc} is the cylinder volume at TDC position, and V_{ivc_eff} is the effective cylinder volume where the in-cylinder compressed air pressure is extrapolated to be identical to the intake manifold pressure [43,44].

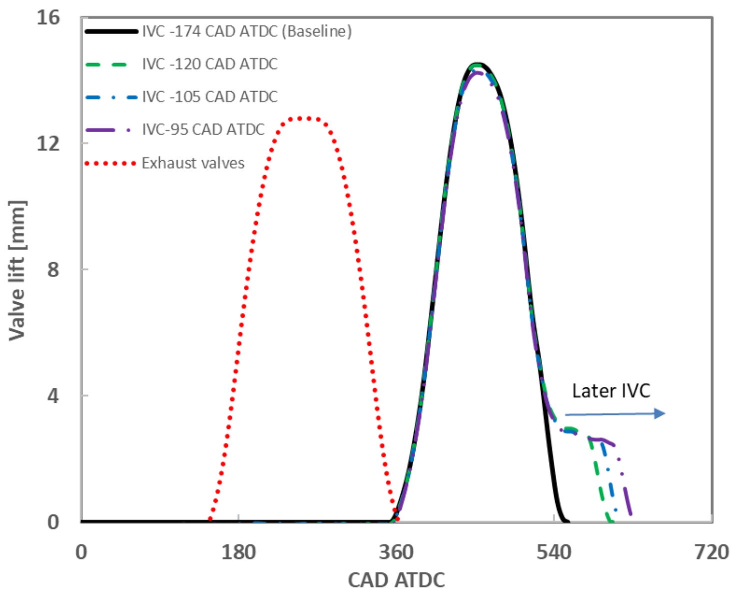

Figure 2. Fixed exhaust and variable intake valve lift profiles.

2.3 Intake and exhaust systems

As depicted in Figure 1, the compressed air was supplied by an external supercharger with closed loop control. The intake mass flow rate was measured by a thermal mass flow meter. Two large surge tanks were installed in the intake and exhaust systems to damp out the pressure fluctuations in the intake and exhaust manifolds resulted from the gas exchange dynamics of the engine. Both instantaneous intake and exhaust manifold pressures were measured by piezo-resistive pressure transducers. The intake manifold pressure was fine adjusted by an intake throttle valve while the exhaust back pressure was independently controlled through a butterfly valve located downstream of the exhaust surge tank. External cooled EGR was introduced into the engine using a pulse width modulation controlled poppet valve installed upstream of the intake surge tank, and the pressure differential between the intake and exhaust manifolds. Engine coolant and lubrication oil were supplied externally and their temperatures along with the intake air and EGR flow temperatures were controlled by the water cooled heat exchangers.

2.4 Fuel delivery system

During the experiments, the diesel fuel was injected into the engine by a high-pressure solenoid injector through a high pressure pump and a common rail with a maximum fuel pressure of

2200 bar. A dedicated electronic control unit (ECU) was used to control fuel injection parameters such as injection pressure, start of injection (SOI), and the number of injections per cycle. The fuel consumption was determined by measuring the total fuel supplied to and from the high pressure pump and diesel injector via two Coriolis flow meters.

2.5 Exhaust emissions measurement

A Horiba MEXA-7170 DEGR emission analyser was used to measure exhaust gases (NOx, HC, CO, and carbon dioxide (CO_2)). To allow for high pressure sampling and avoid condensation, a high pressure sampling module and a heated line were used between the exhaust sampling point and the emission analyser. The smoke number was measured downstream of the exhaust back pressure valve using an AVL 415SE Smoke Meter, and thereafter converted from filter smoke number (FSN) to mg/m^3 [45]. All the exhaust gas components were converted to net indicated specific gas emissions (in g/kWh) according to [46]. In this study, the EGR rate was defined as the ratio of the measured CO_2 concentration in the intake surge tank ($(CO_2\%)_{intake}$) to the CO_2 concentration in the exhaust manifold ($(CO_2\%)_{exhaust}$) as

$$EGR\ rate = \frac{(CO_2\%)_{intake}}{(CO_2\%)_{exhaust}} * 100\% \tag{2}$$

2.6 Engine test data analysis

The instantaneous in-cylinder pressure was measured by a piezo-electric pressure transducer with a sampling revolution of 0.5 CAD. The in-cylinder pressure data was recorded through a charge amplifier and was averaged over 200 engine cycles to calculate the apparent heat release rate (HRR). According to [1], the apparent HRR was calculated as

$$HRR = \frac{\gamma}{(\gamma-1)}\, p\, \frac{dV}{d\theta} + \frac{1}{(\gamma-1)}\, V\, \frac{dp}{d\theta} \tag{3}$$

where γ is defined as the ratio of specific heats and assumeed constant at 1.33 throughout the engine cycle; V and p are the in-cylinder volume and pressure, respectively; θ is the crank angle.

In this study, the CA10, CA50 (combustion phasing) and CA90 were defined as the crank angle when the fuel mass fraction burned (MFB) reached 10%, 50%, and 90%, respectively. Ignition delay was defined as the period between the SOI and the start of combustion (SOC), denoted as 0.3% MFB point of the average cycle. The combustion stability was measured by the coefficient of variation of the IMEP (COV_IMEP) over the sampled cycles.

3. Methodology

3.1 Engine operation

The experimental work was carried out at a speed of 1250 rpm and a low engine load of 6 bar IMEP. Figure 3 shows the operation points of WHSC for HD diesel engines. The size of the circle represents the weighting factor. A larger circle indicates a higher relative weight of the engine operation condition over the WHSC cycle. As shown in Figure 3, the test point is located in a high residency area of a typical HD diesel engine drive cycle, representing an engine operating condition where exhaust gas temperature is low and exhaust emissions such as NOx and soot are relatively high.

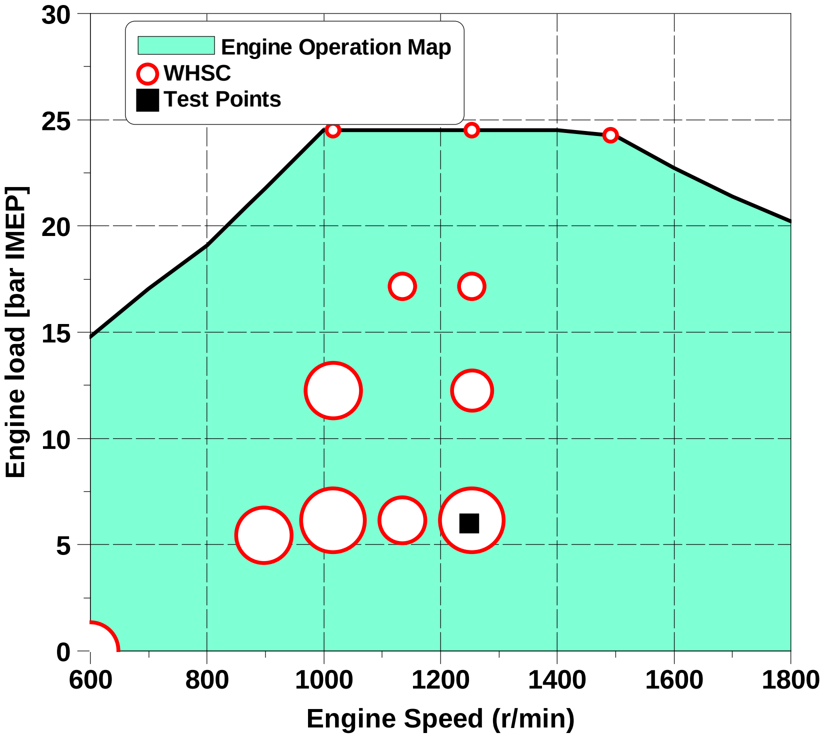

Figure 3. Experimental test point and WHSC operation conditions over an estimated HD diesel engine speed-load map.

Table 2 summaries the engine operating conditions for the different combustion control strategies investigated. The effect of Miller cycle was studied with two LIVC settings and three intake pressures. The ECR was decreased from 16.8 to13.5 and 12.5 for the Miller cycle cases. In the case of combined use of Miller cycle and EGR, the in-cylinder air flow mass was decreased noticeable, resulting in poor combustion instability and excessive smoke. Therefore, a moderate EGR rate of 15% along with an ECR of 13.5 were employed when the EGR was combined with the Miler cycle. Finally, the combined effect of Miller cycler, EGR and post injection was evaluated at two ECRs of 13.5 and 14.5 and 15% EGR.

Table 2. Engine operating conditions for the different combustion control strategies. (? Add SOI valves)

Parameter	Value			
Speed	1250 rpm			
Load	6 bar IMEP			
Injection pressure	1160 bar			
Intake temperature	303 ± 1K			
Testing modes	Baseline	Miller cycle	Miller cycle + EGR	Miller cycle + EGR + Post injection

Intake pressure	1.44 bar	1.44, 1.64, and 1.84 bar	1.44 bar	1.44 bar
Exhaust pressure	0.10 bar higher than the intake pressure			
IVC timing	-174 CAD ATDC	-95, -105 CAD ATDC	-105 CAD ATDC	-120 and -105 CAD ATDC
ECR	16.8	13.5 and 12.5	13.5	14.5 and 13.5
EGR	0%	0%	15%	15%
Post fuel injection	No	No	No	Yes

During the experiments, a small pilot injection of 3 mm^3 with a constant dwell time of 1 ms prior to the main injection timing was employed in order to keep the maximum pressure rise rate (PRR) below 20 bar/CAD. The SOI of main injection was optimised to give the maximum fuel conversion efficiency at each operating condition. The coolant and oil temperatures were kept within 358 ± 2 K. Oil pressure was maintained within 4.0 ± 0.1 bar. Stable engine operation was determined by controlling the COV_IMEP below 3%. The specifications of measurement equipment can be found in Appendix A.

3.2 Engine Modelling and Validation

In order to better analyse the influence of Miller cycle, EGR, and post injection on in-cylinder combustion process, a 1D thermodynamic simulation has been carried out using Ricardo Wave software to estimate the mean in-cylinder gas temperatures and burned zone gas temperatures. This software use finite difference method to solve the 1D unsteady compressible flow equations, including conservation of mass, momentum and energy [47].

The geometric dimensions of intake and exhaust pipes and surge tanks were accurately measured from the engine bench while the ports and valve flow coefficients were provided by the engine supplier. The combustion process was simulated by using the experimentally derived heat release rate profile based on the measured in-cylinder pressure. The heat transfer was calculated by the Woschni heat transfer model [48], which assumes a simple convective heat transfer from a confined volume surrounded on all sides by cylinder walls. The thermodynamic state of the in-cylinder gas was estimated considering the interactions among the enthalpy of fluxes in and out of the chamber, heat transfer, and piston work by using a two zone model, as proposed by Saegusa et al. [49].

The calculated intake air mass flow rate, IMEP, in-cylinder pressure, intake and exhaust manifold pressures were calibrated against the experimental data. In all cases, the maximum pressure is validated to within 3% of the experimental data and the modelled and experimental values for average intake and exhaust manifold pressures were computed to be within 1.5%. Figure 4 shows the in-cylinder pressure while Figure 5 shows the intake and exhaust pressures. The pressure variations in the intake and exhaust systems are primarily due to the piston velocity, valve open area variation, and the unsteady gas-flow effects that result from these geometric variations. The primary frequency in both the intake and exhaust corresponds to the frequency of the intake and exhaust processes [1]. Results showed that there is a good agreement between the simulated and experimental results of in-cylinder pressure as well as intake and exhaust pressures for the “Miller cycle + EGR” strategy. Thus, the validated1D engine model could be used to calculate T_m and T_b.

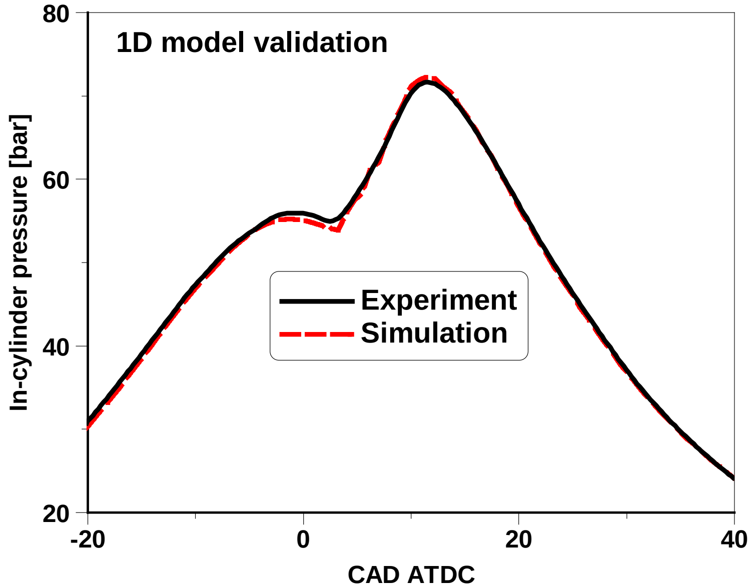

Figure 4. Experimental and simulated in-cylinder pressures for the “Miller cycle + EGR” strategy.

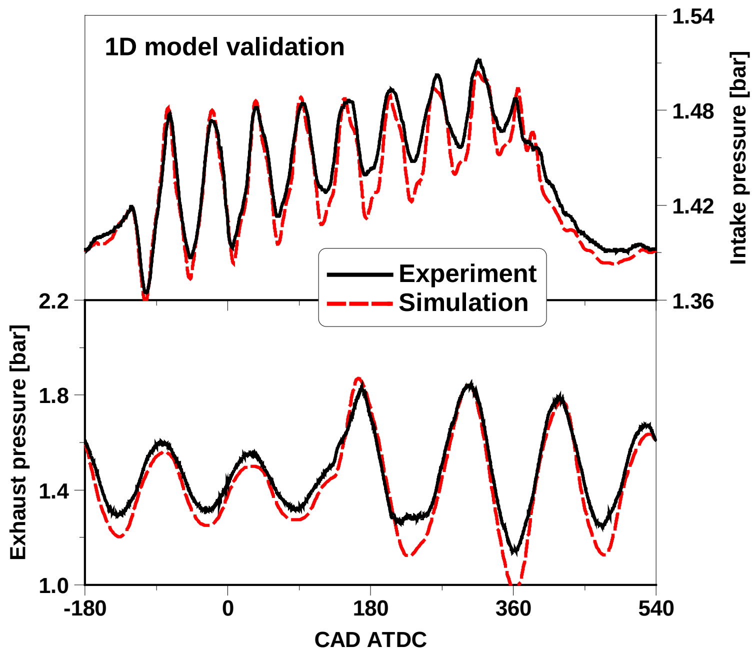

Figure 5. Experimental and simulated intake and exhaust manifold pressures for the “Miller cycle + EGR” strategy.

4. Results and discussion

The experimental results were divided into four sections. In the first section, the isolated effect of Miller cycle under three intake pressures (P_{int}) is investigated. This is followed by an investigation of the effect of Miller cycle combined with EGR for NOx reduction. The third section shows the potential of post injection to minimise soot and CO emissions from the "Miller cycle + EGR" strategy. Finally, the effectiveness of the "Miller cycle + EGR + post injection" strategy for emissions and EGT control at low engine load was evaluated by means of a cost-benefit and overall exhaust emissions analysis.

4.1 The effect of Miller cycle and boost pressure

Figure 6 shows the in-cylinder pressure, HRR, and injector signal for the baseline engine operation and Miller cycle cases (IVC at -95 CAD ATDC) with a constant main SOI at -4 CAD ATDC. Figure 7 depicts T_m and T_b, which were calculated using the 1D engine thermodynamic model. The intake pressure for the Miller cycle strategy was varied between 1.44 bar (e.g. same P_{int} as the baseline) and 1.84 bar (e.g. same lambda as the baseline).

The Miller cycle case with a constant P_{int} of 1.44 bar (red dashed line) was characterised by a significantly lower in-cylinder pressure and a higher degree of premixed combustion as suggested by the appearance of the pre-mixed heat release before the main heat release process. This was the result of the lower ECR, which decreased the compressed air pressure and temperature and increased the ignition delay.

Relatively higher in-cylinder pressure and peak HRR were observed when increasing the P_{int} of the Miller cycle cases due to the higher in-cylinder charge density. The first peak heat release disappeared as a result of the higher compression pressure and earlier SOC. The Miller cycle strategy with higher intake pressure achieved a similar HRR profile to the baseline case when operating with the same lambda. It is important to note that the in-cylinder gas pressure was slightly lower than that of the baseline case. This was a result of the lower in-cylinder gas temperatures achieved by this Miller cycle case with a P_{int} of 1.84 bar.

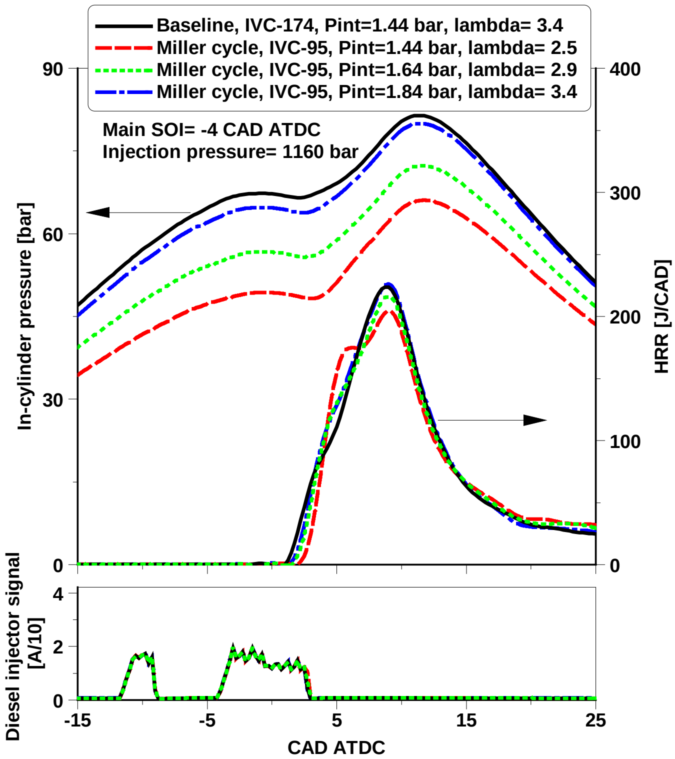

Figure 6. In-cylinder pressure, HRR, and diesel injection signal for the baseline and Miller cycle cases.

The application of Miller cycle decreased the compressed air temperature by approximately 30 K because of the LIVC and lower ECR. However, the Miller cycle operation with constant P_{int} of 1.44 bar reduced the in-cylinder fresh charge and hence the total heat capacity, leading to a higher mean gas temperature, T_m , as reported in our previous work [26] and by Benajes et al. [40] with EIVC. When operating with the same lambda, the peak of the mean gas temperature T_m decreased with increased P_{int} and was lower than that of the baseline case. The burned gas temperature, T_b , decreased slightly with the use of Miller cycle due to the lower compressed gas temperatures (e.g. prior to the SOC). A relatively higher T_b after SOC was observed in the Miller cycle case with a constant P_{int} of 1.44 bar due to lower in-cylinder mass, as indicated by the lambda.

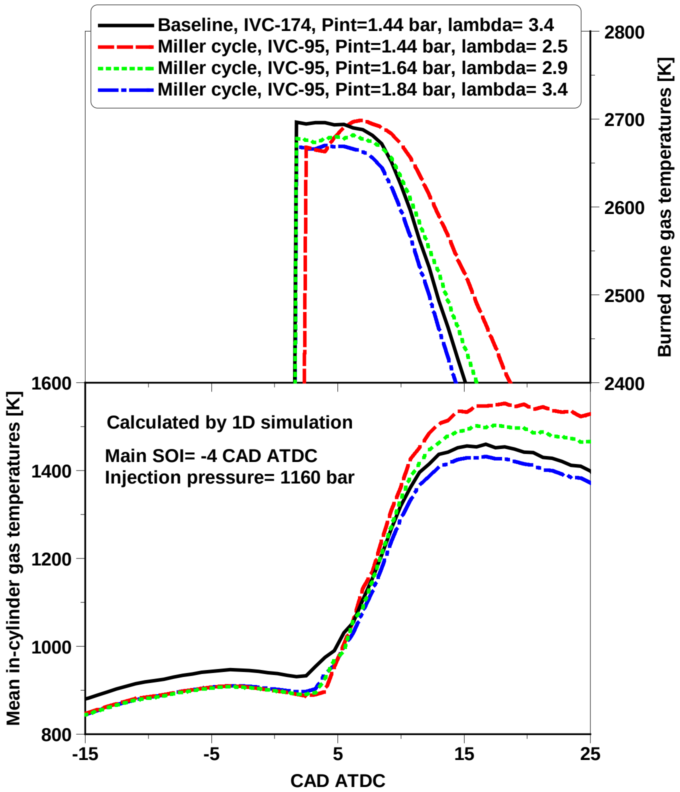

Figure 7. Calculated mean in-cylinder gas temperatures and burned zone temperatures for the baseline and Miller cycle cases.

Figure 8 shows the CA50, CA90, CA50-CA90, and combustion duration (CA10-CA90) over a sweep of main SOI. There was little difference in CA50 of the baseline and Miller cycle cases at a given main SOI. The Miller cycle with a P_{int} of 1.44 bar delayed the CA90 due to the later ignition and slowed down combustion process in the late combustion phase. This resulted in a relatively longer period time of CA50-CA90 as well as combustion duration. At the same lambda, the higher P_{int} improved the in-cylinder oxygen availability, which helped accelerate the combustion process. As a result, the CA90 was advanced and thus a shorter period time of CA50-CA90 and combustion duration. As a result, the combustion characteristics of the Miller cycle was similar to that of the baseline condition when operating with the same lambda.

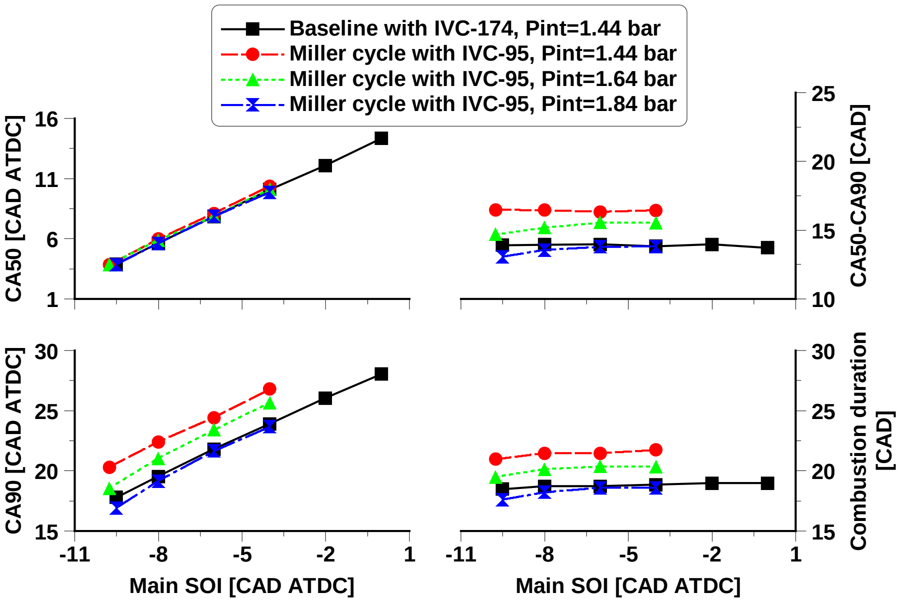

Figure 8. The effect of Miller cycle on combustion characteristics.

Figure 9 depicts engine performance parameters and net indicated specific emissions. The use of Miller cycle with a constant P_{int} of 1.44 bar significantly reduced the lambda value due to lower in-cylinder mass trapped. This was also the reason for the 75 K increase in the EGT, which is an important achievement considering that the EGT of 539 K of the baseline case was probably insufficiently high for efficient aftertreatment operation. According to [50], the optimum performance of the ATS is achieved when the inlet temperature at ATS is maintained between 523 K and 723 K. It is also important to note that the EGT showed in this study is the engine-out temperature, which will be further reduced downstream of the turbocharger in a production multi-cylinder engine.

The net indicated efficiency of the Miller cycle at a P_{int} of 1.44 bar was decreased by approximately 1% in comparison with the baseline engine operation. This was attributed to the extended CA50-CA90 period and longer total combustion duration, and higher heat losses to cylinder walls due to higher T_m (see Figure 7). The use of higher P_{int} to maintain the in-cylinder lambda value helped increasing the net indicated efficiency due to the higher in-cylinder oxygen availability, but adversely affected the gains obtained in terms of EGT and NOx emissions. Miller cycle operation with a P_{int} of 1.84 bar achieved a net indicated efficiency as high as the baseline case.

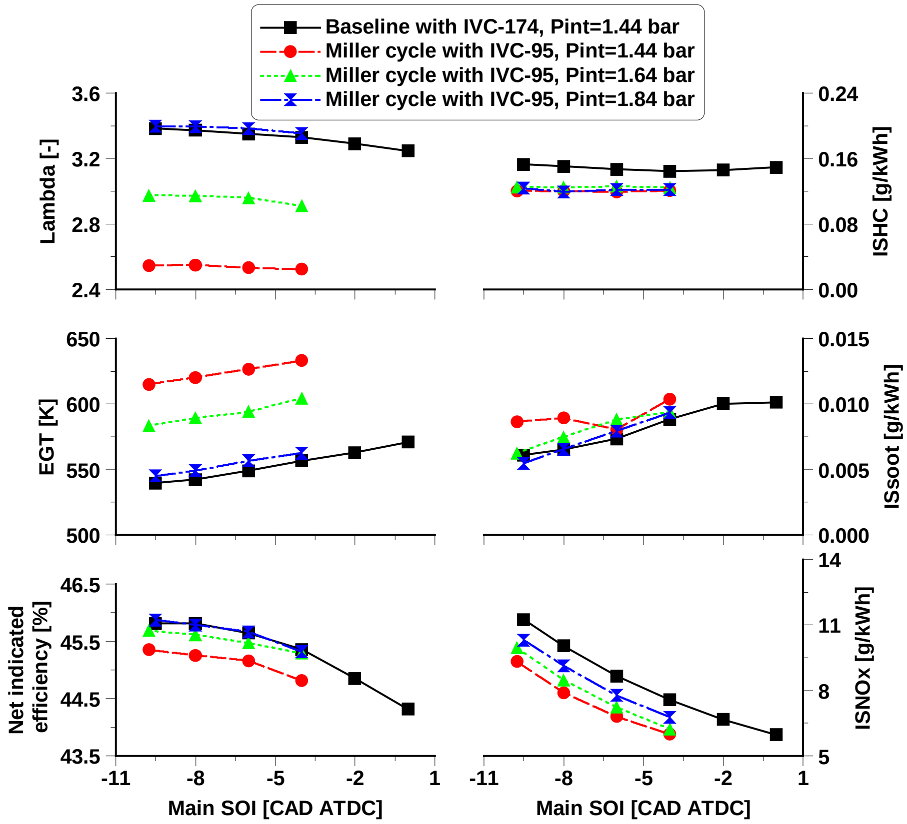

Figure 9. The effect of Miller cycle on engine performance and exhaust emissions.

The Miller cycle operation reduced the NOx emissions by 21% to 6 g/kWh at the expense of slightly higher soot emissions. This was primarily a result of the lower in-cylinder air mass trapped and reduced initial burned zone gas temperature. Later main SOI effectively decreased combustion temperatures and therefore NOx emissions. As the P_{int} of the Miller cycle cases was increased, soot emissions were reduced and NOx emissions increased. It can also be seen from Figure 9 that the application of Miller cycle decreased unburned HC emissions, regardless of the intake pressure used. This was possibly attributed to the relatively lower lambda and higher T_m, which can improve the oxidation rates during the expansion stroke.

The above results have shown that Miller cycle was effective in the EGT management and NOx emissions control but at the expense of lower net indicated efficiency. Despite the improvements in the net indicated efficiency obtained when increasing the P_{int}, a higher lambda can impair the EGT and the NOx emissions benefits introduced by the Miller cycle strategy. In addition, it should be noted that a conventional turbocharging system is likely not able to deliver the required airflow rate at such low load operations. For this reason, a more sophisticated boosting system, such as a two-stage variable geometry turbocharger configuration, would be needed [51,52].

4.2 The combined effect of Miller cycle with EGR

EGR was introduced to the Miller cycle operation in order to further reduce the engine-out NOx levels, as it is an effective and well established technology for NOx emissions control from internal combustion engines [34,53,54]. As explained previously, ECR was set at 13.5 to maintain the combustion stability. Considering the fact that a higher levels of P_{int} might not be achievable in a turbocharged multi-cylinder engine operating at low load condition [55], the P_{int} was kept at 1.44 bar.

Figure 10 shows the in-cylinder pressure, HRR, and injector signal for the Miller cycle cases with and without EGR with a constant main SOI at -4 CAD ATDC. The addition of EGR delayed the SOC due to the lower in-cylinder oxygen concentration (dilution effect) and lower compression temperature because of the lower specific heat values [34]. This increased the degree of premixed combustion and decreased both the peak HRR and peak in-cylinder pressure.

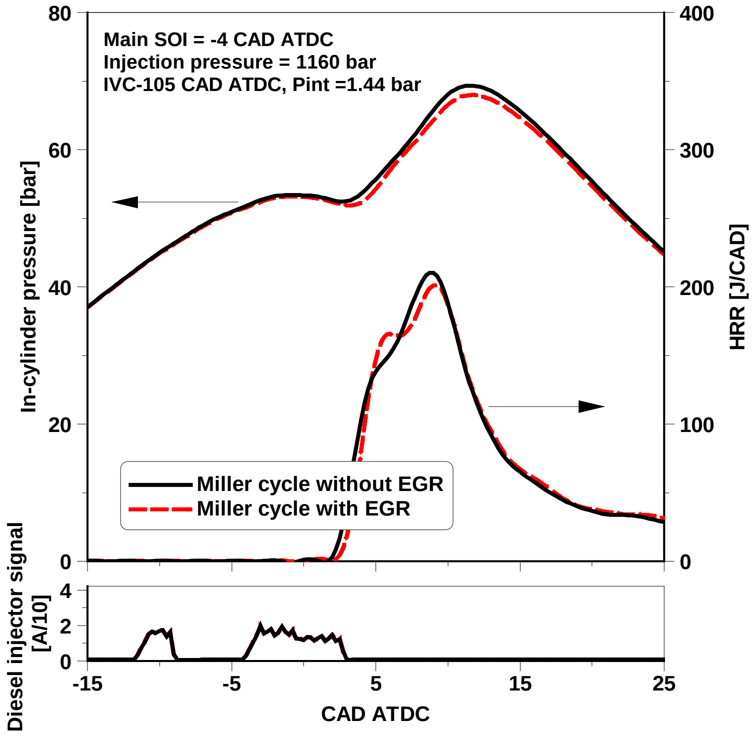

Figure 10. In-cylinder pressure, HRR, and diesel injector signal for Miller cycle cases with and without EGR.

Figure 11 depicts the burned zone gas temperatures and mean in-cylinder gas temperatures calculated using the 1D engine model. The dilution effect and higher heat capacity (thermal effect) introduced by EGR decreased the T_b by more than 100 K, consequently helping to curb NOx formation. No significant differences in the T_m curves were observed when comparing the Miller cycle cases with and without EGR.

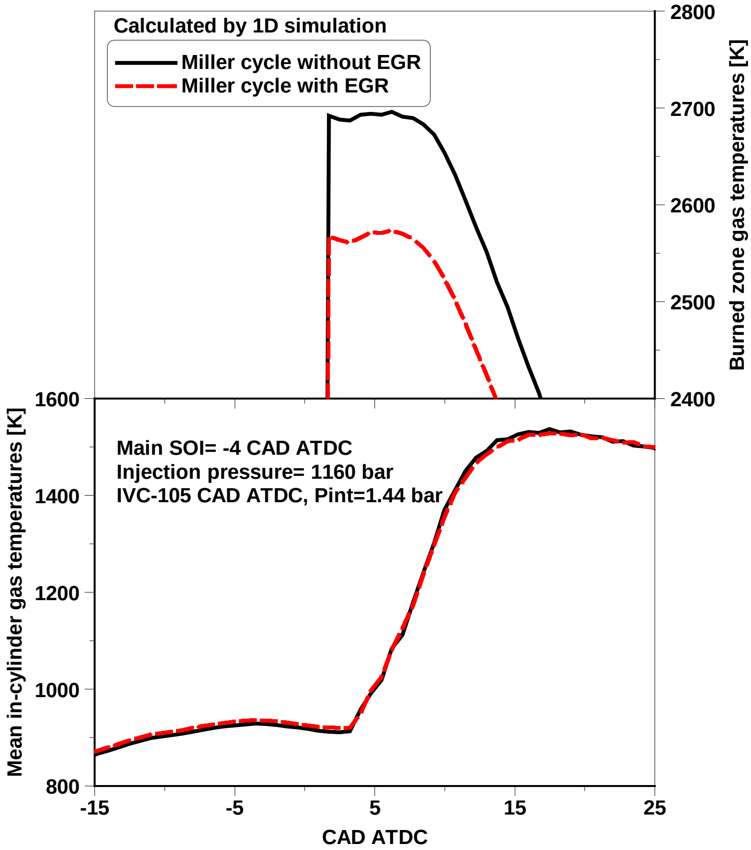

Figure 11. Calculated mean in-cylinder gas temperatures and burned zone gas temperatures for Miller cycle cases with and without EGR.

Figure 12 shows the resulting heat release characteristics. The addition of EGR to a Miller cycle operation had little impact on the CA50, but slowed down the late combustion process (e.g. delayed CA90). This was a result of the later SOC and the lower in-cylinder oxygen concentration. The combination of these effects with a lower peak T_b yielded a longer period of CA50-CA90, as well as increased the total combustion duration (CA10-CA90) by up to 3 CAD when compared to the Miller cycle cases without EGR.

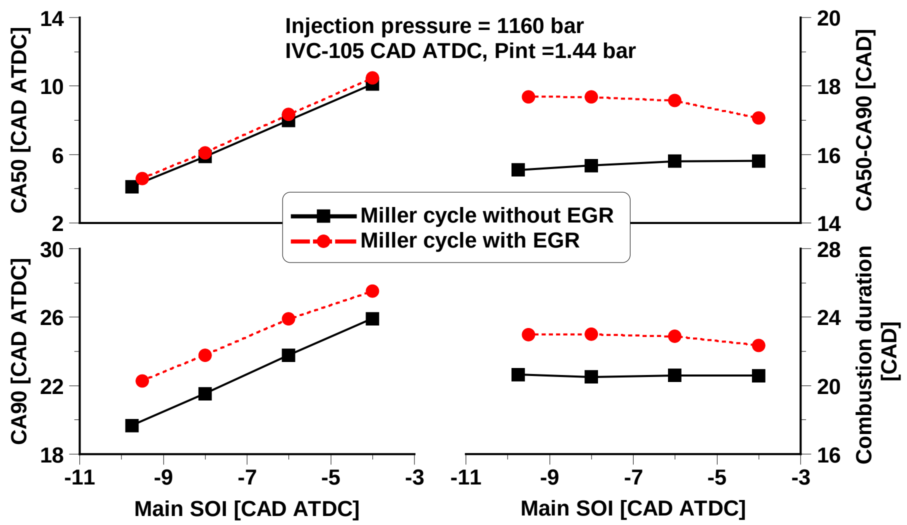

Figure 12. The effect of EGR on combustion characteristics of Miller cycle cases.

Figure 13 depicts the engine performance parameters and net indicated specific emissions. The use of EGR decreased the lambda, which contributed to an increase of approximately 7 K in the EGT. Additionally, the lower T_b and in-cylinder oxygen concentration for the conditions with 15% EGR curbed the NOx emissions by up to 58%. However, the later and longer combustion process of the Miller cycle cases with EGR decreased the net indicated efficiency by up to 0.8% and significantly increased soot and CO emissions. These results can limit the potential of the "Miller cycle + EGR" strategy for efficient and clean low load engine operation.

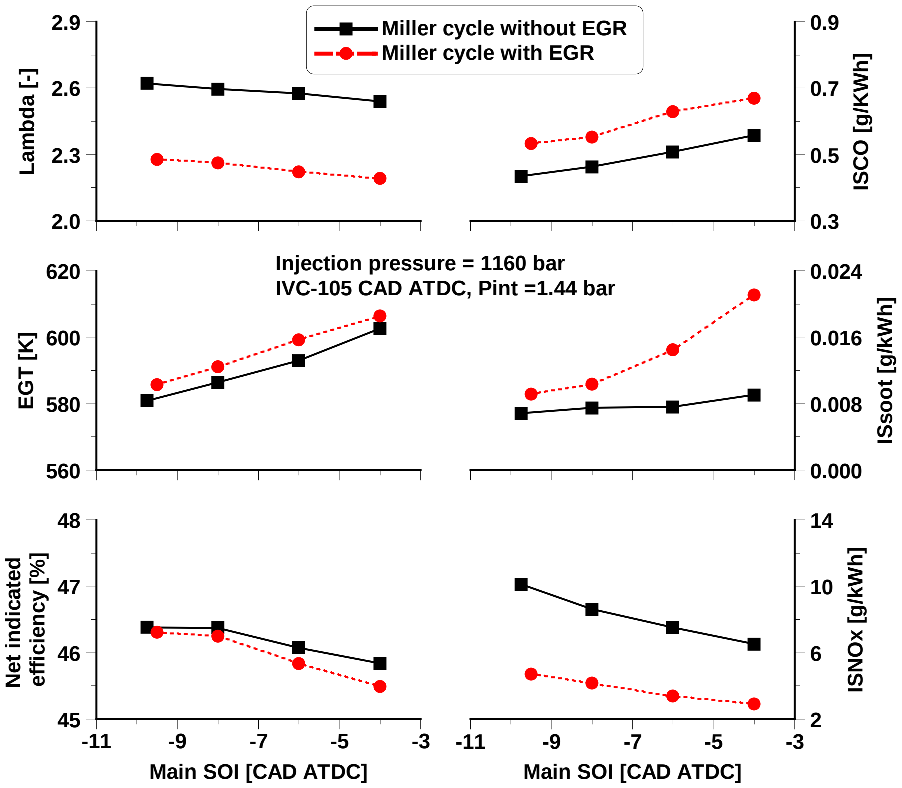

Figure 13. The effect of EGR on engine performance and exhaust emissions of Miller cycle cases.

4.3 Exploring the potential of a post injection strategy

The use of post injections has been demonstrated as an effective means of mitigating soot and CO emissions [56,57]. Therefore, the post injection strategy was investigated in an attempt to improve upon the performance and emissions of the "Miller cycle + EGR" strategy.

4.3.1 The optimization of the post injection

Before analysing the potential of the "Miller cycle + EGR + post injection" strategy, the post injection timing and fuel quantity were optimised in order to achieve high efficiency and low engine-out emissions. The optimization was carried out at three IVC timings, including the baseline at -174 CAD ATDC and Miller cycle cases at -120 and -105 CAD ATDC. The main SOI was held constant at -4 CAD ATDC. At a given post injection timing, a sweep of post injection quantity of 6, 9, 12, 15 mm^3 (equivalent to 7%, 11%, 15%, and 20% of the total fuel injection quantity, respectively) was performed.

Firstly, the post injection timing was varied between 15 and 24 CAD ATDC while the quantity was held constant at 9 mm^3. Figure 14 shows that the soot emissions were sensitive to the post injection timing, decreasing initially and increasing significantly with the most retarded post injection timings. This was likely attributed to the trade-off effect of post injected fuel on soot formation and oxidation rates in the late combustion phase [56]. Meanwhile, changes in the post injection timing resulted in little impact on NOx emissions. Overall, the post injection timing of 18 CAD ATDC achieved the lowest soot emissions with relatively small decrease in net indicated efficiency, and thus was selected for the post injection quantity sweep.

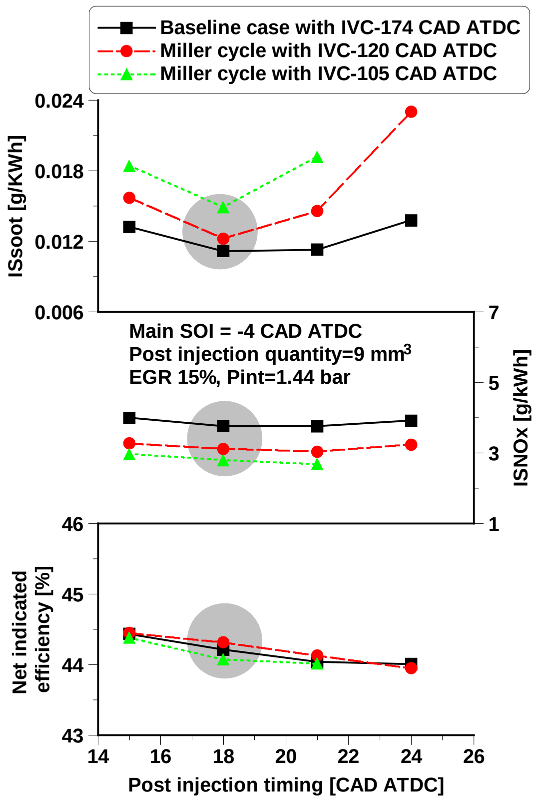

Figure 14. Optimization of the post injection timing.

Figure 15 depicts the optimization of the post injection quantity while maintaining the post injection timing constant at 18 CAD ATDC. An increase in the post injection quantity reduced soot and NOx emissions at the expense of a reduction in the net indicated efficiency, regardless of the IVC timing. A post injection quantity of 12 mm^3 achieved the optimum trade-off between engine performance and emissions. Therefore, the next subsection explores the potential of the

"Miller cycle + EGR + post injection" strategy using a post injection of 12 mm^3 at 18 CAD ATDC.

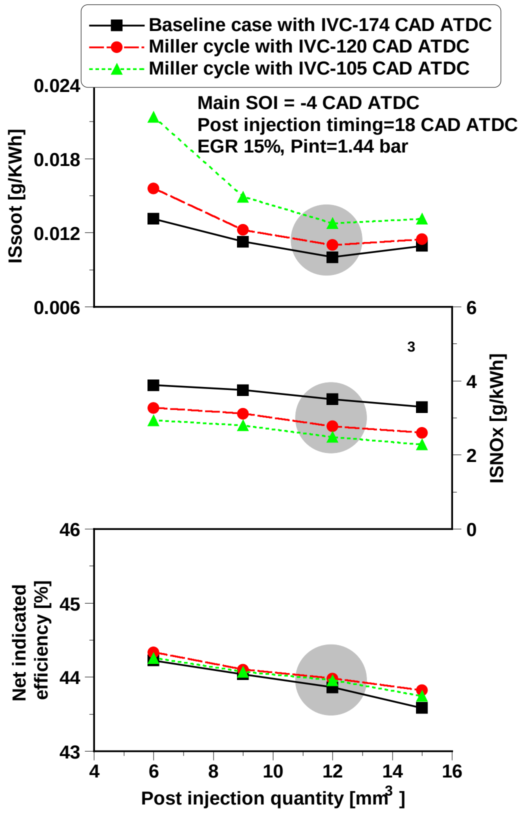

Figure 15. Optimization of the post injection quantity.

4.3.2 The combined effect of the post injection with Miller cycle and EGR

Figure 16 depicts the in-cylinder pressure, HRR, and injector signal for the baseline and Miller cycle cases with and without the optimized post injection strategy. The use of post injection yielded a second and late peak HRR, which represented the combustion of the post injected fuel. The decreased fuel mass in the main injection consequently, lowered the first peak HRR and thus the peak in-cylinder pressure when compared to the baseline cases. Figure 17 shows that the post injection strategy also decreased the peak mean in-cylinder gas temperature but increased the average temperature during the late stages of the combustion process. Additionally, it can be seen that the relatively richer mixture of the Miller cycle cases (e.g. lower lambda at a constant P_{int}) shortened the ignition delay of the post injected fuel in comparison with that of the baseline case with a post injection.

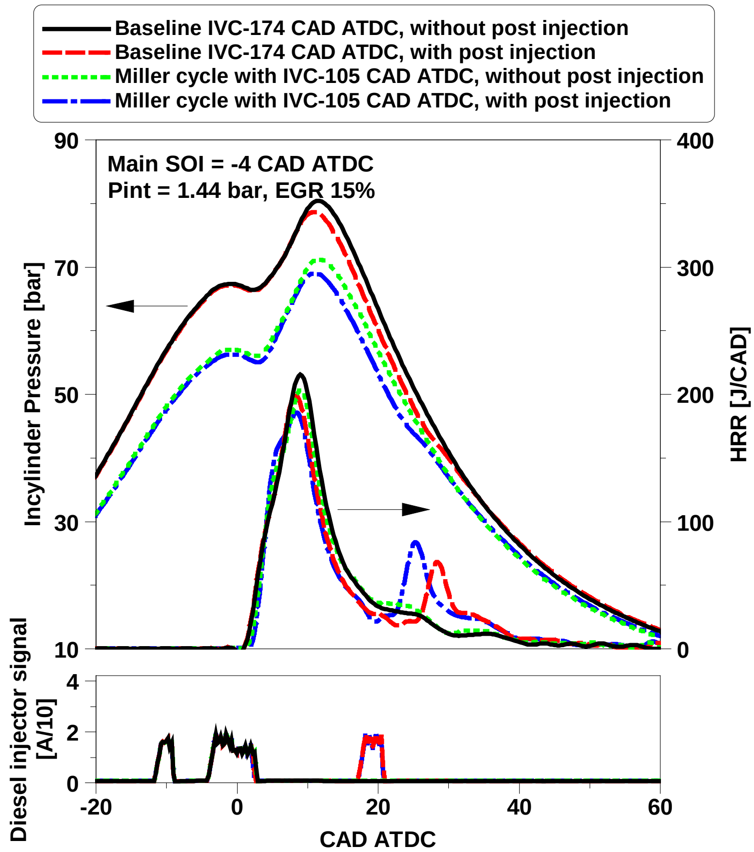

Figure 16. In-cylinder pressure, HRR, and diesel injector signal for the baseline and Miller cycle cases with and without post injection.

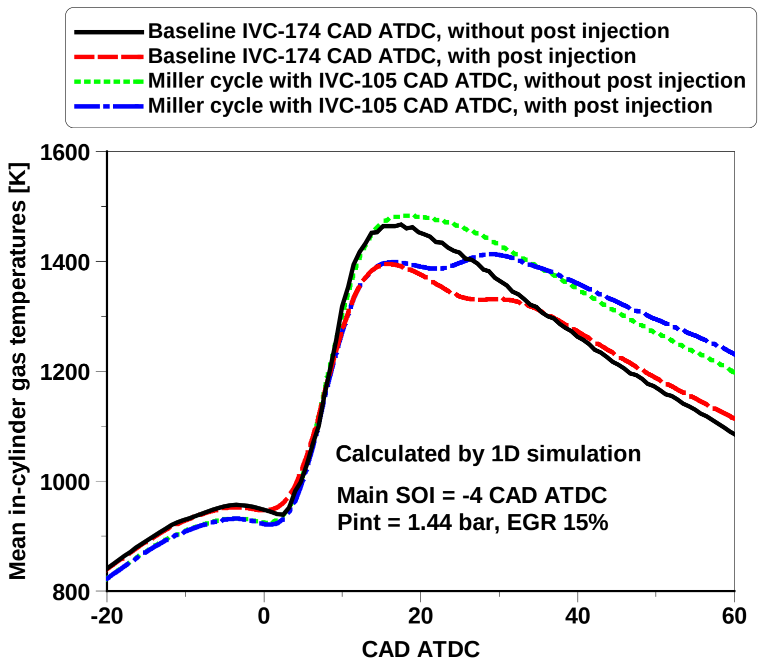

Figure 17. Calculated mean in-cylinder gas temperatures for the baseline and Miller cycle cases with and without post injection.

Figure 18 compares the resulting heat release characteristics for different IVC timings with and without post injection. The addition of the post injection delayed the CA50 and CA90 as more fuel was burned during a relatively colder and later combustion phase. As a result, the period of CA50-CA90 was longer for the cases with post injection. These effects contributed to an increase in the combustion duration by up to 5 CAD when compared to the cases without post injection.

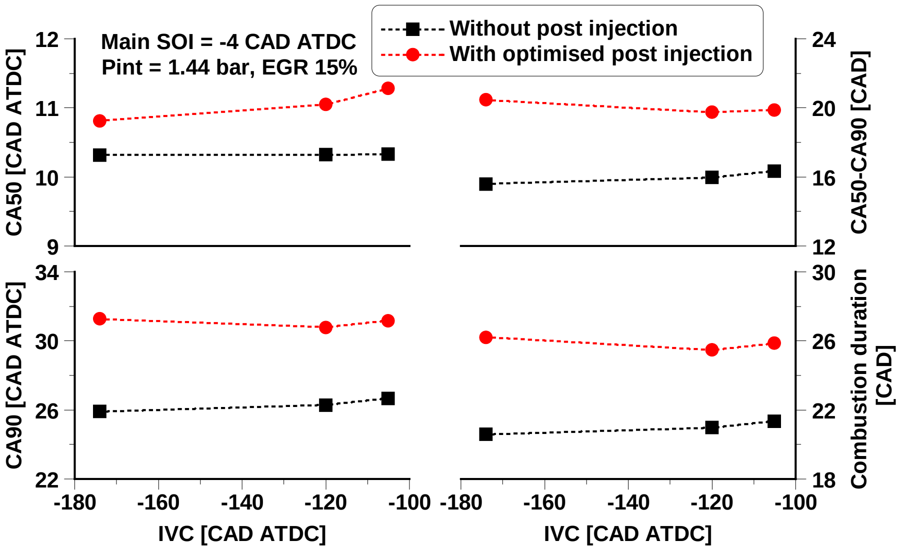

Figure 18. The effect of post injection on combustion characteristics.

Figure 19 shows the lambda was slightly reduced and EGT was increased with the addition of post injection. This was because part of diesel fuel was consumed later in the cycle and consequently a decrease in net indicated efficiency. Nevertheless, the difference of net indicated efficiency penalty between the cases with and without post injection was reduced with delayed IVC timing, decreasing from 1.6% at the baseline IVC to below 1% in the Miller cycle with IVC-105 CAD ATDC. This was probably due to the relatively faster heat release of the post injected fuel in the Miller cycle cases.

The emission results showed that soot emissions were significantly reduced by the post injection. The primary reasons for this improvement are likely the shorter injection durations, the enhanced fuel-air mixing, and the increased late combustion temperature achieved with the multiple injections [57]. Meanwhile, the use of a post injection led to a reduction in NOx emissions of 20% on average. This was due to the lower lambda (e.g. less oxygen availability) and most likely the lower burned zone gas temperatures achieved with this injection strategy. The levels of CO showed a similar trend to the soot emissions, and were also reduced with the post injection strategy attributed to the increased late combustion temperatures.

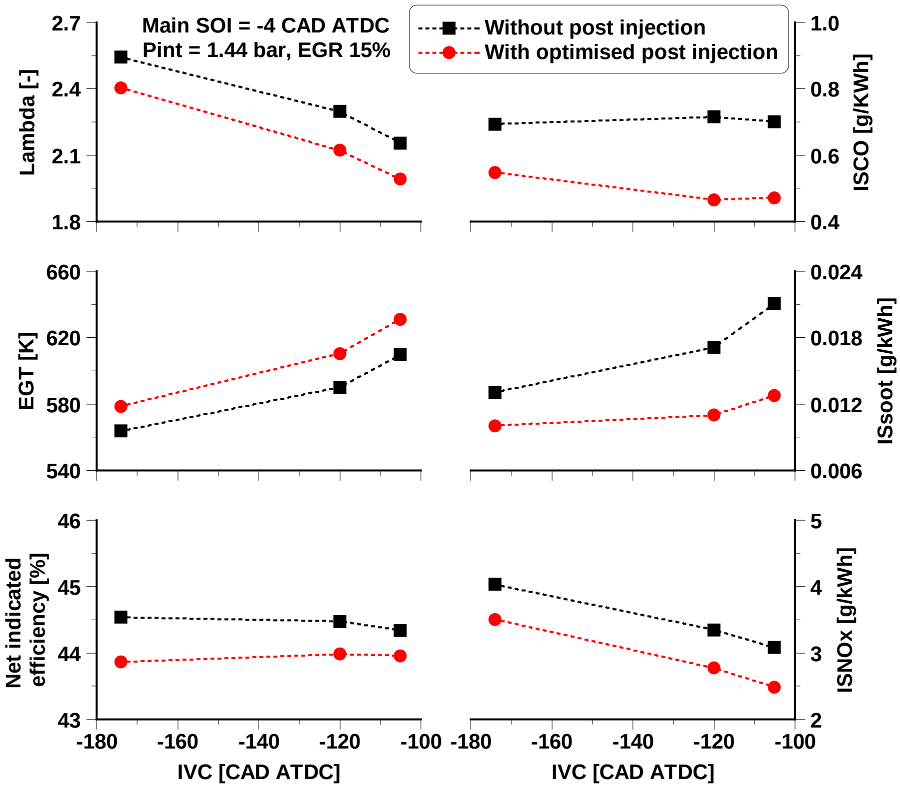

Figure 19. The effect of post injection on engine performance and exhaust emissions.

4.4 Cost-benefit and overall analysis

In this section, the total fluid consumption ($\dot{m}_{total}$) was calculated by summing the measured diesel flow rate ($\dot{m}_{diesel}$) and aqueous urea solution consumption in an SCR system ($\dot{m}_{urea}$), which allowed for a cost-benefit and overall emissions analysis of the different combustion control strategies.

$$\dot{m}_{total} = \dot{m}_{urea} + \dot{m}_{diesel} \quad (4)$$

Since the urea consumption in the SCR system depends on the operating conditions as well as engine-out NOx emissions, reductions in the levels of engine-out NOx can help minimise the urea flow rate. According to [58,59], the urea consumption in the SCR system can be estimated as 1% of the diesel equivalent fuel flow per g/kWh of NOx reduction necessary to meet the Euro VI limit (NOx_{EuroVI}) of 0.4 g/kWh.

$$\dot{\mathrm{m}}_{urea} = 0.01\,(\mathrm{ISNOx} - \mathrm{NOx}_{EuroVI})\,\dot{\mathrm{m}}_{diesel} \tag{5}$$

which is then used in the calculation of the corrected total fluid efficiency

$$\text{Corrected total fluid efficiency} = \frac{P_i}{\dot{\mathrm{m}}_{total}\,\mathrm{LHV}_{diesel}} \tag{6}$$

where P_i is the net indicated power and LHV_{diesel} is the diesel lower heating value of 42.9 MJ/kg.

Figure 20 provides an overall assessment of the potential of Miller cycle with EGR and post injection to improve upon the EGT, exhaust emissions, and engine operational cost of a diesel engine operating at low load. The results of various advanced combustion control strategies are compared to the baseline case using a constant main SOI of -4 CAD ATDC and P_{int} of 1.44 bar. Additionally, all Miller cycle cases were operated with a same IVC at -105 CAD ATDC in order to allow a fair comparison.

Compared to the baseline case, a “Miller cycle-only” strategy decreased NOx emissions by 14% accompanied with an increase of 47 K in EGT. This was achieved at the expense of a reduction of 0.3% in the net indicated fuel conversion efficiency. The combination of a Miller cycle strategy with EGR achieved better improvement in NOx emissions and EGT, decreasing NOx emissions by 58% and increasing EGT by 54 K in comparison with the baseline case. This significant improvement was obtained with a reduction of 1.1% in the net indicated fuel conversion efficiency. However, the “Miller cycle + EGR” strategy increased soot emissions significantly from 0.009 g/kWh in the baseline case to 0.022 g/kWh and also increased CO emissions by 8%. The introduction of a post injection helped control soot and CO emissions, allowed for further reductions in NOx emissions and increased the EGT by 75 K. It can be also seen that all advanced combustion control strategies achieved relatively lower levels of HC emissions than that of the baseline case. As discussed in Section 4.3, the later and longer combustion process of the “Miller cycle + EGR + post injection” strategy adversely affected net indicated fuel conversion efficiency, decreasing it by 1.9% when compared with the baseline engine operation.

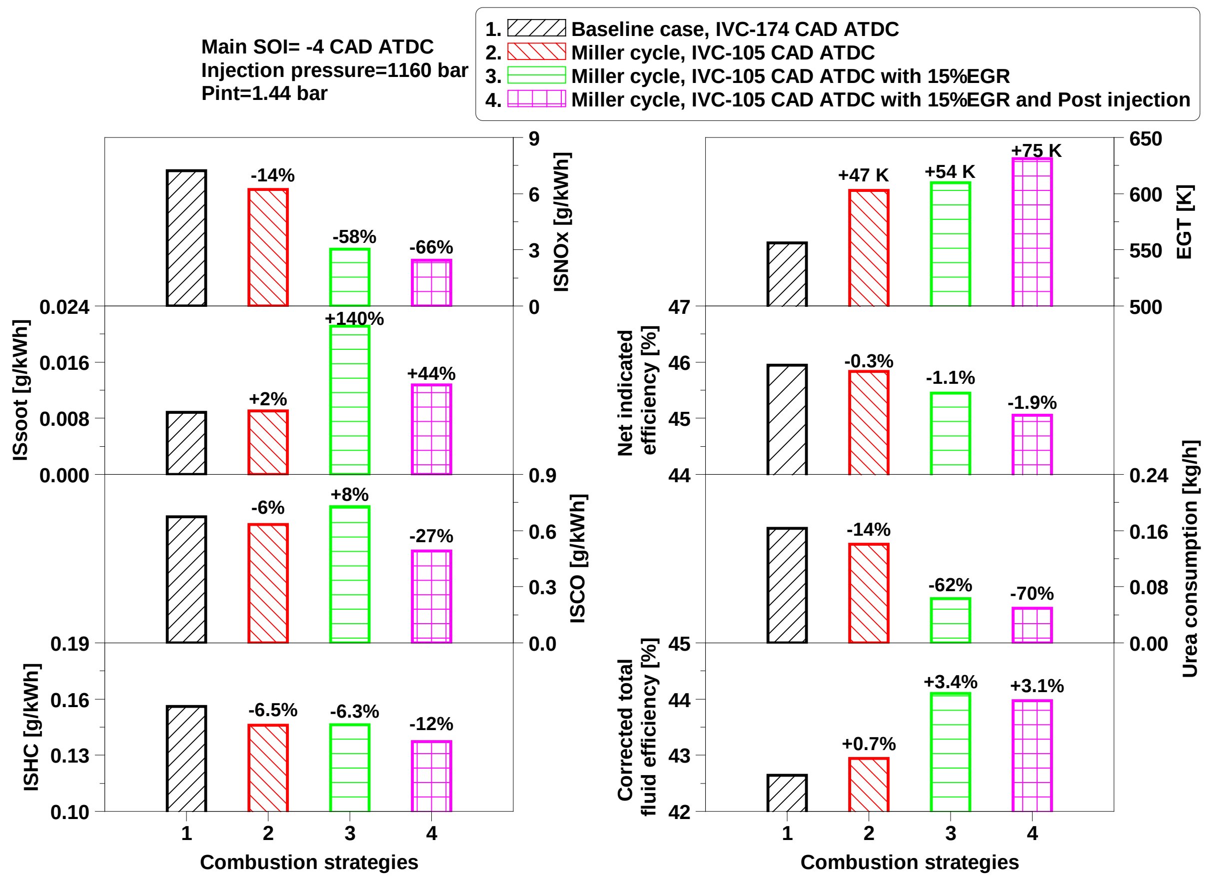

Figure 20. Cost-benefit and overall emissions for various combustion control strategies.

Figure 20 also revealed that the advanced combustion control strategies helped decrease the urea consumption via lower engine-out NOx emissions. This minimised the total fluid consumption and therefore increased the corrected total fluid efficiency, despite a lower net indicated efficiency. The highest improvement in corrected total fluid efficiency of 3.4% was achieved by the “Miller cycle + EGR” strategy as a result of the high NOx reduction capability combined with a relatively lower net indicated efficiency penalty. Alternatively, the “Miller cycle + EGR + post injection” strategy increased the corrected total fluid efficiency by 3.1% while improving upon EGT as well as soot and CO emissions. Therefore, the combined strategy of “Miller cycle + EGR + post injection” was identified as the most effective means to achieve low engine operational cost and enable exhaust emissions and EGT control.

5. Conclusions

This study investigated the effect of a Miller cycle-only strategy as well as Miller cycle operations combined with EGR and post injection on the combustion process, exhaust emissions, and performance of a HD diesel engine. The aim of the research was to identify an effective combustion control strategy for exhaust emissions and exhaust gas temperatures control, in order to minimise the combined consumption of fuel and urea solution at a low engine load of 6 bar IMEP. Miller cycle, EGR, and multiple injections were achieved by means of a VVA system, a high-pressure loop cooled EGR, and a common rail fuel injection system, respectively. A 1D simulation was used for the calculation of the mean in-cylinder gas temperatures and burned zone gas temperatures, improving the analysis and discussion. The main findings can be summarized as follows:

1. A Miller cycle-only strategy with IVC at -95 CAD ATDC increased the EGT by 75 K and reduced NOx emissions by 21%, but with a penalty of 1% in the net indicated fuel

conversion efficiency when operating the engine with the same intake pressure as the baseline case. This was due to the reduced in-cylinder charge mass and lower peak combustion temperature.

2. A higher intake pressure to keep the in-cylinder air/fuel ratio constant allowed for improvements in the net indicated fuel conversion efficiency and soot emissions of a Miller cycle operation at the expense of a reduction in the NOx and EGT benefits.
3. The “Miller cycle + EGR” strategy enabled lower burned zone gas temperatures, significantly reducing NOx emissions. However, the lower combustion temperatures and lambda (e.g. in-cylinder oxygen availability) adversely affected soot and CO emissions.
4. The addition of a post injection was effective in minimising soot and CO emissions of the “Miller cycle + EGR” strategy while achieving lower NOx emissions and higher EGT. The improvements, however, were achieved at the expense of a decrease in net indicated fuel conversion efficiency.
5. Overall, the “Miller cycle + EGR + post injection” strategy was identified as the most effective means for exhaust emissions and EGT control among the various approaches examined in this study. This combination of combustion control strategies reduced engine-out NOx emissions by 66% and increased the EGT by 75K, which in turn resulted in an increased in the corrected total fluid efficiency by 3.1%. Furthermore, the use of this combined strategy with a 12 mm^3 post injection at 18 CAD ATDC helped attain simultaneous low levels of soot, CO and HC emissions.

Contact information

Wei Guan
Wei.guan@brunel.ac.uk
gwei916@163.com
Centre for Advanced Powertrain and Fuels Research
College of Engineering, Design and Physical Sciences
Brunel University London

Kingston Lane
Uxbridge
Middlesex UB8 3PH
United Kingdom

Acknowledgments

The first author, Mr W Guan, would like to acknowledge the Guangxi Yuchai Machinery Company for supporting his PhD study supervised by Prof. Hua Zhao at Brunel University London.

Declaration of conflicting interests

The author(s) declared no potential conflicts of interest with respect to the research, authorship, and/or publication of this article.

Funding

The author(s) disclosed receipt of the following financial support for the research, authorship, and/or publication of this article: Funding for this project was provided by Guangxi Yuchai Machinery Company.

Definitions/Abbreviations

ATDC	After Firing Top Dead Center.
ATS	Aftertreatment System.
CA10	Crank Angle of 10% Cumulative Heat Release.
CA50	Crank Angle of 50% Cumulative Heat Release.
CA90	Crank Angle of 90% Cumulative Heat Release.
CAD	Crank Angle Degree.
CO	Carbon Monoxide.
CO_2	Carbon Dioxide.
COV_IMEP	Coefficient of Variation of IMEP.
$(CO_2\%)_{intake}$	CO_2 concentration in the intake manifold.
$(CO_2\%)_{exhaust}$	CO_2 concentration in the exhaust manifold.
DOC	Diesel Oxidation Catalyst.
DPF	Diesel Particulate Filter.
ECR	Effective Compression Ratio.
ECU	Electronic Control Unit.

EGR	Exhaust Gas Recirculation.
EGT	Exhaust Gas Temperatures.
EEVO	Early Exhaust Valve Opening.
FSN	Filter Smoke Number.
HCCI	Homogenous Charge Compression Ignition.
HRR	Heat Release Rate.
HC	Hydrocarbons.
HD	Heavy-duty.
IMEP	Indicated Mean Effective Pressure.
IVO	Intake Valve Opening.
IVC	Intake Valve Closing
ISFC	Net Indicated Specific Fuel Consumption.
ISSoot	Net Indicated Specific Emissions of Soot.
ISNOx	Net Indicated Specific Emissions of NOx.
ISCO	Net Indicated Specific Emissions of CO.
ISHC	Net Indicated Specific Emissions of Unburned HC.
LTC	Low Temperature Combustion.
LIVC	Late Intake Valve Closing.
$\dot{m}_{urea}$	Aqueous Urea Solution Consumption
$\dot{m}_{total}$	Total Fluid Consumption
$\dot{m}_{diesel}$	Diesel Flow Rate
NOx	Nitrogen Oxides.
1D	One Dimensional
PCCI	Premixed Charge Compression Ignition.
P_{int}	Intake Pressure.
PPCI	Partially Premixed Charge Compression Ignition.
PRR	Pressure Rise Rate.
SCR	Selective Catalytic Reduction.
SOI	Start of Injection.
SOC	Start of Combustion.
TDC	Firing Top Dead Centre.
T_m	Mean In-cylinder Gas Temperatures.
T_b	Burned Zone Gas Temperatures.

VVA Variable Valve Actuation.

WHSC World Harmonized Stationary Cycle

References

1. Heywood J.B, “Internal Combustion Engine Fundamentals,” ISBN 007028637X, 1988.
2. Environmental Protection Agency, National Highway Traffic Safety Administration, and Department of Transportation, “Greenhouse Gas Emissions and Fuel Efficiency Standards for Medium- and Heavy-Duty Engines and Vehicles - Phase 2,” 1–1690, 2016.
3. Bendu, H. and Murugan, S., “Homogeneous charge compression ignition (HCCI) combustion: Mixture preparation and control strategies in diesel engines,” *Renew. Sustain. Energy Rev.* 38:732–746, 2014, doi:10.1016/j.rser.2014.07.019.
4. Neely, G.D., Sasaki, S., Huang, Y., Leet, J.A., and Stewart, D.W., “New Diesel Emission Control Strategy to Meet US Tier 2 Emissions Regulations,” 2005(724), 2005, doi:10.4271/2005-01-1091.
5. Musculus, M.P.B., Miles, P.C., and Pickett, L.M., “Conceptual models for partially premixed low-temperature diesel combustion,” Elsevier Ltd, ISBN 0360-1285, 2013, doi:10.1016/j.pecs.2012.09.001.
6. Shi, L., Zhang, L., Deng, K., Lv, X., and Fang, J., “Experimental Research on Mixture Distribution of Diesel Premixed Low-Temperature Combustion,” 8, 2015, doi:10.4271/2015-01-1839.
7. Dev, S., Chaudhari, H.B., Gothekar, S., Juttu, S., Walke, H., and Marathe, N. V, “Review on Advanced Low Temperature Combustion Approach for BS VI,” 2017, doi:10.4271/2017-26-0042.Copyright.
8. Gehrke, S., Kovács, D., Eilts, P., Rempel, A., and Eckert, P., “Investigation of VVA-Based Exhaust Management Strategies by Means of a HD Single Cylinder Research Engine and Rapid Prototyping Systems,” *SAE Tech. Pap.* 01(0587):47–61, 2013, doi:10.4271/2013-01-0587.
9. Bai, S., Chen, G., Sun, Q., Wang, G., and Li, G. xiang, “Influence of active control strategies on exhaust thermal management for diesel particular filter active regeneration,” *Appl. Therm. Eng.* 119:297–303, 2017, doi:10.1016/j.applthermaleng.2017.03.012.
10. Buckendale, L.R., Stanton, D.W., and Stanton, D.W., “Systematic Development of Highly Efficient and Clean Engines to Meet Future Commercial Vehicle Greenhouse Gas Regulations,” *SAE Int.* 2013-01-2421, 2013, doi:10.4271/2013-01-2421.
11. Goto, T., Hatamura, K., Takizawa, S., Hayama, N., Abe, H., and Kanesaka, H., “Development of V6 Miller Cycle Gasoline Engine,” (41 2), 1994, doi:10.4271/940198.
12. Akima, K., Seko, K., Taga, W., Torii, K., and Nakamura, S., “Development of New Low Fuel Consumption 1.8L i-VTEC Gasoline Engine with Delayed Intake Valve Closing,” 2006(724), 2006, doi:10.4271/2006-01-0192.
13. K. Kishi and T. Satou, “The new Nissan high efficient 1.2L 3cyl GDI Supercharged Engine enables 95g/km CO2 emissions and high driving performance,” *Int. Wiener Mot. 2012*, 2012.
14. Rinaldini, C.A., Mattarelli, E., and Golovitchev, V.I., “Potential of the Miller cycle on a HSDI

diesel automotive engine," *Appl. Energy* 112(x):102–119, 2013, doi:10.1016/j.apenergy.2013.05.056.

15. Scania, "Six new engines added to Scania's Euro 6 Range," https://www.scania.com/group/en/wp-%0Acontent/uploads/sites/2/2017/06/p17067en-six-new-engines-added-to- scanias-euro-6-range, 2017.

16. Kim, J. and Bae, C., "An investigation on the effects of late intake valve closing and exhaust gas recirculation in a single-cylinder research diesel engine in the low-load condition," *Proc. Inst. Mech. Eng. Part D J. Automob. Eng.* 230(6):771–787, 2015, doi:10.1177/0954407015595149.

17. https://www.dieselnet.com/tech/engine_miller-cycle.php.

18. Miller, R., "Supercharged Engine," USA Patent 2817322, 1957.

19. Fukuzawa, Y., Shimoda, H., and Kakuhama, Y., "Development of high efficiency Miller cycle gas engine," *Tech. Rev.* 38(3):146–150, 2001.

20. He, X., Durrett, R.P., and Sun, Z., "Late Intake Valve Closing as an Emissions Control Strategy at Tier 2 Bin 5 Engine-Out NOx Level," *SAE Int. J. Engines* 1(1):2008-01–0637, 2008, doi:10.4271/2008-01-0637.

21. J. BENAJES , S. MOLINA, R.N. and M.R., "IMPROVING POLLUTANT EMISSIONS IN DIESEL ENGINES FOR HEAVY-DUTY TRANSPORTATION USING RETARDED INTAKE VALVE CLOSING STRATEGIES," *Int. J. …* 13(2):293–300, 2012, doi:10.1007/s12239.

22. Bruce Morey, "IAV brings variable valvetrains to heavy duty," *SAE Int. United States*, 2017.

23. Molina, S., García, A., Monsalve-Serrano, J., and Estepa, D., "Miller cycle for improved efficiency, load range and emissions in a heavy-duty engine running under reactivity controlled compression ignition combustion," *Appl. Therm. Eng.* 136(December 2017):161–168, 2018, doi:10.1016/j.applthermaleng.2018.02.106.

24. Gonca, G., Sahin, B., Parlak, A., Ust, Y., Ayhan, V., Cesur, I., and Boru, B., "Theoretical and experimental investigation of the Miller cycle diesel engine in terms of performance and emission parameters," *Appl. Energy* 138:11–20, 2015, doi:10.1016/j.apenergy.2014.10.043.

25. Wang, Y., Zeng, S., Huang, J., He, Y., Huang, X., Lin, L., and Li, S., "Experimental investigation of applying Miller cycle to reduce NOxemission from diesel engine," *Proc. Inst. Mech. Eng. Part A J. Power Energy* 219(8):631–638, 2005, doi:10.1243/095765005X31289.

26. Guan, W., Pedrozo, V., Zhao, H., Ban, Z., and Lin, T., "Investigation of EGR and Miller Cycle for NOx Emissions and Exhaust Temperature Control of a Heavy-Duty Diesel Engine," *SAE Tech. Pap.*, 2017, doi:10.4271/2017-01-2227.

27. Gonca, G., Sahin, B., Parlak, A., Ayhan, V., Cesur, I., and Koksal, S., "Application of the Miller cycle and turbo charging into a diesel engine to improve performance and decrease NO emissions," *Energy* 93:795–800, 2015, doi:10.1016/j.energy.2015.08.032.

28. Wu, B., Zhan, Q., Yu, X., Lv, G., Nie, X., and Liu, S., "Effects of Miller cycle and variable geometry turbocharger on combustion and emissions in steady and transient cold process," *Appl. Therm. Eng.* 118(x):621–629, 2017, doi:10.1016/j.applthermaleng.2017.02.074.

29. Guan, W., Zhao, H., Ban, Z., and Lin, T., "Exploring alternative combustion control strategies for low-load exhaust gas temperature management of a heavy-duty diesel engine," *Int. J. Engine Res.* 146808741875558, 2018, doi:10.1177/1468087418755586.

30. Ding, C., Roberts, L., Fain, D.J., Ramesh, A.K., Shaver, G.M., McCarthy, J., Ruth, M., Koeberlein, E., Holloway, E.A., and Nielsen, D., "Fuel efficient exhaust thermal management for compression ignition engines during idle via cylinder deactivation and flexible valve actuation," *Int. J. Engine Res.* 17(6):619–630, 2016, doi:10.1177/1468087415597413.

31. Ratzberger, R., Kraxner, T., Pramhas, J., Hadl, K., Eichlseder, H., and Buergler, L., "Evaluation of Valve Train Variability in Diesel Engines," *SAE Int. J. Engines* 8(5):2015-24–2532, 2015, doi:10.4271/2015-24-2532.

32. Garg, A., Magee, M., Ding, C., Roberts, L., Shaver, G., Koeberlein, E., Shute, R., Koeberlein, D., McCarthy, J., and Nielsen, D., "Fuel-efficient exhaust thermal management using cylinder throttling via intake valve closing timing modulation," *Proc. Inst. Mech. Eng. Part D J. Automob. Eng.* 230(4):470–478, 2016, doi:10.1177/0954407015586896.

33. Benajes, J., Molina, S., Novella, R., and Belarte, E., "Evaluation of massive exhaust gas recirculation and Miller cycle strategies for mixing-controlled low temperature combustion in a heavy duty diesel engine," *Energy* 71:355–366, 2014, doi:10.1016/j.energy.2014.04.083.

34. Asad, U. and Zheng, M., "Exhaust gas recirculation for advanced diesel combustion cycles," *Appl. Energy* 123:242–252, 2014, doi:10.1016/j.apenergy.2014.02.073.

35. Ladommatos, N., Abdelhalim, S.M., Zhao, H., and Hu, Z., "The Dilution, Chemical, and Thermal Effects of Exhaust Gas Recirculation on Diesel Engine Emissions - Part 2: Effects of Carbon Dioxide," *Proc. Inst. Mech. Eng. Part D* 212(January 1998):25–42, 1996, doi:10.4271/961167.

36. Zhao, C., Yu, G., Yang, J., Bai, M., and Shang, F., "Achievement of Diesel Low Temperature Combustion through Higher Boost and EGR Control Coupled with Miller Cycle," (x), 2015, doi:10.4271/2015-01-0383.

37. Sjöblom, J., "Combined Effects of Late IVC and EGR on Low-load Diesel Combustion," *SAE Int. J. Engines* 8(1):2014-01-2878, 2014, doi:10.4271/2014-01-2878.

38. Benajes, J., Molina, S., Martín, J., and Novella, R., "Effect of advancing the closing angle of the intake valves on diffusion-controlled combustion in a HD diesel engine," *Appl. Therm. Eng.* 29(10):1947–1954, 2009, doi:10.1016/j.applthermaleng.2008.09.014.

39. Martins, M.E.S. and Lanzanova, T.D.M., "Full-load Miller cycle with ethanol and EGR: Potential benefits and challenges," *Appl. Therm. Eng.* 90:274–285, 2015, doi:10.1016/j.applthermaleng.2015.06.086.

40. Benajes, J., Serrano, J.R., Molina, S., and Novella, R., "Potential of Atkinson cycle combined with EGR for pollutant control in a HD diesel engine," *Energy Convers. Manag.* 50(1):174–183, 2009, doi:10.1016/j.enconman.2008.08.034.

41. Verschaeren, R., Schaepdryver, W., Serruys, T., Bastiaen, M., Vervaeke, L., and Verhelst, S., "Experimental study of NOx reduction on a medium speed heavy duty diesel engine by the application of EGR (exhaust gas recirculation) and Miller timing," *Energy* 76(x):614–621, 2014, doi:10.1016/j.energy.2014.08.059.

42. Authorities, A., "Acts Adopted By Bodies Created By International Agreements," *Off. J. Eur. Union* 7–9, 2013.

43. Stricker, K., Kocher, L., Koeberlein, E., Alstine, D. Van, and Shaver, G.M., "Estimation of effective compression ratio for engines utilizing flexible intake valve actuation," *Proc. Inst. Mech. Eng. Part D J. Automob. Eng.* 226(8):1001–1015, 2012, doi:10.1177/0954407012438024.

44. Pedrozo, V., “An experimental study of ethanol-diesel dual-fuel combustion for high efficiency and clean heavy-duty engines,” PhD Thesis, Brunel University London, 2017.

45. AVL., “AVL 415SE Smoke Meter,” *Prod. Guid. Graz, Austria;*, 2013.

46. Regulation No 49 – uniform provisions concerning the measures to be taken against the emission of gaseous and particulate pollutants from compression-ignition engines and positive ignition engines for use in vehicles. Off J Eur Union, 2013.

47. Ricardo WAVE software. http://www.software.ricardo.com/products/wave.

48. Woschni, G., A Universally Applicable Equation for the Instantaneous Heat Transfer Coefficient in the Internal Combustion Engine, 1967, doi:10.4271/670931.

49. Saegusa, Y., Tanaka, J., and Korematsu, K., “Prediction and Measurement of Combustion Limit of Gaseous Fuel Mixed with Air in Intake Pipe of Diesel Engines,” *Pap. Pap. 1990-2002* (412), 1995, doi:10.4271/930759.

50. Lambert, C., Hammerle, R., and Mcgill, R., “Technical Advantages of Urea SCR for Light-Duty and Heavy-Duty Diesel Vehicle Applications Reprinted From : Diesel Exhaust Emission Control,” *SAE Tech. Pap.* (724), 2004, doi:10.4271/2004-01-1292.

51. Zhao, J., “Research and application of over-expansion cycle (Atkinson and Miller) engines – A review,” *Appl. Energy* 185:300–319, 2017, doi:10.1016/j.apenergy.2016.10.063.

52. Martins, M.E.S. and Lanzanova, T.D.M., “Full-load Miller cycle with ethanol and EGR: Potential benefits and challenges,” *Appl. Therm. Eng.* 90:274–285, 2015, doi:10.1016/j.applthermaleng.2015.06.086.

53. Pedrozo, V.B., May, I., and Zhao, H., “Exploring the mid-load potential of ethanol-diesel dual-fuel combustion with and without EGR,” *Appl. Energy* 193:263–275, 2017, doi:10.1016/j.apenergy.2017.02.043.

54. Hanson, R., Ickes, A., and Wallner, T., “Comparison of RCCI Operation with and without EGR over the Full Operating Map of a Heavy-Duty Diesel Engine,” *SAE Tech. Pap.* (x), 2016, doi:10.4271/2016-01-0794.

55. Modiyani, R., Kocher, L., Alstine, D.G. Van, Koeberlein, E., Stricker, K., Meckl, P., and Shaver, G., “Effect of intake valve closure modulation on effective compression ratio and gas exchange in turbocharged multi-cylinder engines utilizing EGR,” *Int. J. Engine Res.* 12(6):617–631, 2011, doi:10.1177/1468087411415180.

56. Bobba, M., Musculus, M., and Neel, W., “Effect of Post Injections on In-Cylinder and Exhaust Soot for Low-Temperature Combustion in a Heavy- Duty Diesel Engine,” *SAE Int J Engines* 3(1):496–516, 2010, doi:10.4271/2010-01-0612.

57. O’Connor, J. and Musculus, M., “Post Injections for Soot Reduction in Diesel Engines: A Review of Current Understanding,” *SAE Int. J. Engines* 6(1):2013-01–0917, 2013, doi:10.4271/2013-01-0917.

58. Charlton, S., Dollmeyer, T., and Grana, T., “Meeting the US Heavy-Duty EPA 2010 Standards and Providing Increased Value for the Customer,” *SAE Int. J. Commer. Veh.* 3(1):101–110, 2010, doi:10.4271/2010-01-1934.

59. Johnson, T. V, “Diesel Emissions in Review,” *SAE Int. J. Engines* 4(1):143–157, 2011, doi:10.4271/2011-01-0304.

Appendix A. Test cell measurement devices

Variable	Device	Manufacturer	Measurement range	Linearity/Accuracy
Speed	AG 150 Dynamometer	Froude Hofmann	0-8000 rpm	± 1 rpm
Torque	AG 150 Dynamometer	Froude Hofmann	0-500 Nm	± 0.25% of FS
Diesel flow rate (supply)	Proline promass 83A DN01	Endress+Hauser	0-20 kg/h	± 0.10% of reading
Diesel flow rate (return)	Proline promass 83A DN02	Endress+Hauser	0-100 kg/h	± 0.10% of reading
Intake air mass flow rate	Proline t-mass 65F	Endress+Hauser	0-910 kg/h	± 1.5% of reading
In-cylinder pressure	Piezoelectric pressure sensor Type 6125C	Kistler	0-300 bar	≤ ± 0.4% of FS
Intake and exhaust pressures	Piezoresistive pressure sensor Type 4049A	Kistler	0-10 bar	≤ ± 0.5% of FS
Oil pressure	Pressure transducer UNIK 5000	GE	0-10 bar	< ± 0.2% FS
Temperature	Thermocouple K Type	RS	233-1473K	≤ ± 2.5 K
Intake valve lift	S-DVRT-24 Displacement Sensor	LORD MicroStrain	0-24 mm	± 1.0% of reading using straight line
Smoke number	415SE	AVL	0-10 FSN	-
Fuel injector current signal	Current Probe PR30	LEM	0-20A	± 2 mA

Paper Correction

Dear Organizers and Reviewers,

Thank you for your kind comments and suggestions to the manuscript. We have modified the manuscript accordingly, and detailed corrections are listed below point by point. The paragraphs in black are the reviewers' comments, while our responses are listed in blue. All the modifications in the manuscript are highlighted in red.

We look forward to hearing from you.

Sincerely,

Wei Guan

Brunel University London

Reviewer #1

1) The abstract should be reformulated. The abstract is an extremely important and powerful representation of the article. The authors should describe better their research, the main contributions and results, and the conclusions. They have to be direct and highlight the novelty of this study. First paragraph statement is not right and not relevant with the performed work; can be removed.

Thanks, the first paragraph in Abstract has been removed.

2) Introduction:

i) Please avoid lumping references. Instead of lumping refences, please describe in one sentence the most spectacular results of each cited study.

The cited references have been reformulated accordingly in Introduction.

ii) Review should be more critical, rather than a description of previous studies. Following questions must be answered in this literature review:

• How does EGR affect emissions, exhaust temp and volumetric efficiency?

• How does IVC affect emissions, exhaust temp and volumetric efficiency?

• What's the difference between LPEGR and HPEGR? Which strategy is preferred and when?

• Why to combine EGR (LP or HP?) and Miller?

After reading the introduction, the reader must have a clear understanding of the problem.

Thanks for the kind suggestions, the reasons for how do EGR and IVC affect emissions, exhaust temp and volumetric efficiency have been explained accordingly. The type of EGR used is only HP EGR and the difference between LPEGR and HPEGR is not the focus in this work. The reason to combine EGR and Miller cycle is because EGR can effectively curb NOx formation while Miller cycle is a more effective means for exhaust temperature management but with a limited capability for NOx control. Therefore, the combined use of Miller cycle with EGR can achieve high NOx reduction and EGT increase at such low load operation.

iii) Last but not least, what is the research gap that this study bridges? Please highlight the novelty.

There is no such a work investigating the effects of the combination of Miller cycle with EGR and post injection on low load emissions and EGT control. Therefore, this work includes a good novelty and originality. This has been highlighted at the end of Introduction.

iv) A more critical reformulation of the introduction could significantly improve the quality of this study and to get cited more in the future.

Thanks very much for your kind suggestion.

3) Experimental Set-up: Nice presentation of the experimental set up. Few minor comments:

i) Please add error analysis of your data. What’s the RSO of the utilized sensors?

We ensure that the error of all experimental data is controlled below 5% during the study.

Please see attached the Appendix A for the resolution of the primary utilized sensors.

ii) If in-cylinder pressure is monitored, please add that discussion on the document and update figure 1.

Yes, the in-cylinder pressure is monitored and has been shown in Figure 1, which can be seen in the Figure below. The discussion can be seen in Section 2.6.

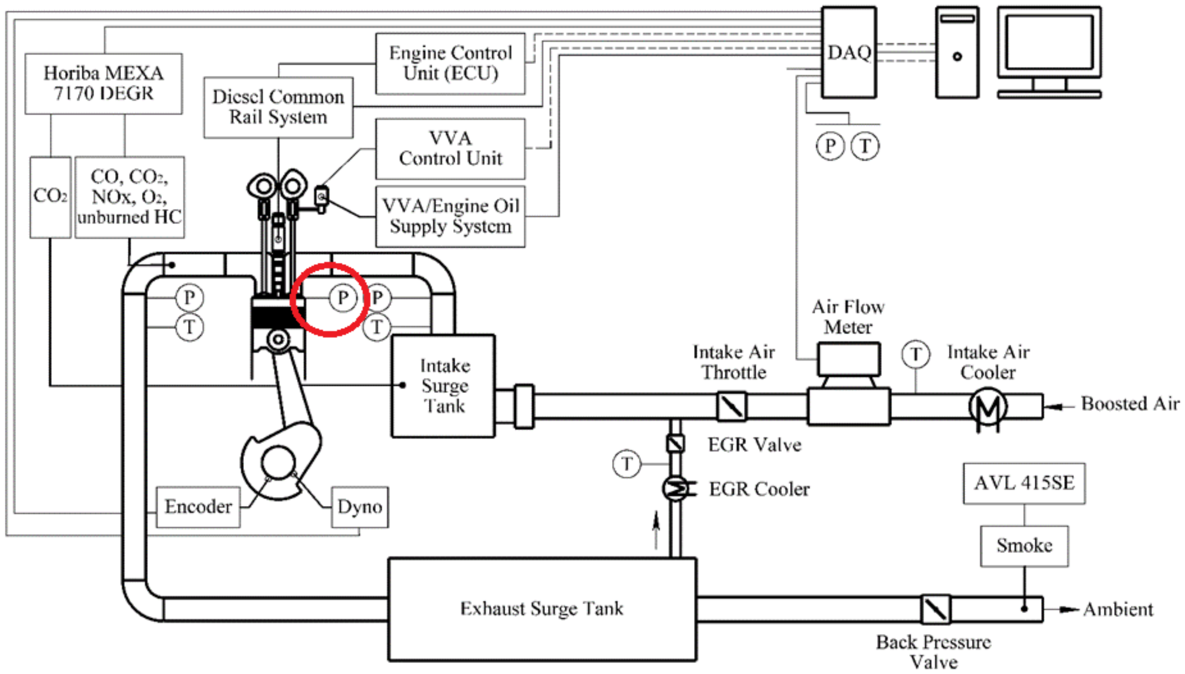

iii) Pg 10, ln 177: please add the full description of ECR in the document and the ECR in parenthesis.

It has been modified accordingly.

iv) Pg 12, ln 222: please provide the value of the specific heat of the polyonymic equation.

Thanks. It has been added accordingly.

4) Methodology: Figure 4: please zoom from 20 to 80 bar range. It seems that the model cannot predict accurately the in-cylinder pressure rise as well as the peak cylinder pressure. Small differences in the pressure trace result much higher error in the predicted heat release rate. What is the error between peak cylinder pressure between sim and exp? Why the authors didn't use a two zone heat release model, presented in many other studies in literature, to calculate burned and unburned temperatures, so as to avoid errors between simulation and experiments? Also error curve vs Cad at figure 5 is important to be added.

In all cases, the maximum pressure is validated to within 3% of the experimental data. The model predicts slightly lower in-cylinder pressures near to the end of compression stroke. This is likely to be a result of over-predicted heat transfer and the fact the modelled in-cylinder pressure is insensitive to the simulated diesel injection pressure.

The model used is a two zone heat release model as presented in Section 3.2. In Figure 5, the modelled and experimental values for average intake and exhaust manifold pressures were computed to be within 1.5%, which has been added in the text.

5) Results:

i) Please express exp data with dots and simulation data with curves when comparison between sim and exp is presented

There is not comparison between simulation and experiment in the Results section. The 1D model was used only to calculate the mean in-cylinder gas temperatures and burned zone gas temperatures once it was validated with the experimental data.

ii) Calculation of temperatures include an error as a result of the deviation between estimated pressure and measured. Please comment that in the text and refer to this error? How much do you expect is that?

Thanks for the kind suggestion. It has been added accordingly in the text in Section 3.2.

iii) The critical point of Miller is boost pressure. Can the results be realistic when conventional turbocharging is applied instead of the external compressor? How does Miller and EGR affect turbocharger operation? What turbocharger design would be required? Please add comments in the text.

Thanks for this good question. These have been added in the text in page 20.

The use of Miller cycle results in less total mixture mass trapped while the introduction of a HP EGR decreased the exhaust flow to pass turbocharger, both which could result in lower turbocharger efficiency. As the Miller degree increases the boost pressure has to accordingly increase in order to maintain the fresh mixture mass trapped. Thus, a conventional supercharging system is not able to deliver the required airflow rate, particularly at low load operations. For this reason, a two-stage variable geometry turbocharger configuration may be very promising but it largely increases the engine complexity. On the other hand, a highly efficient intake intercooler is always needed to cool down the intake air after boosted by a turbocharger.

iv) At session 4.3.2: It would be better to apply only EGR at the baseline scenario and then Miller + EGR to see the effect of Miller. In the way results are presented, the effect of EGR is well known, NOx are reduced because burned temperature is increased and soot is increased. This is what happens at any diesel engine. Please reformulate this chapter and use more data if available.

Thanks for the kind suggestions, the main objective of session 4.3.2 is to estimate the effect of post injection at various IVC timings. Therefore, the EGR rate was maintained constant at 15% for all cases.

v) English and grammar could be reviewed at the results session.

Thanks. The manuscript has been revised and proofread.

vi) Ln 538, pg 32: Could you please add in the discussion the EU limits for any standard off-highway cycle to understand how much higher than the limits this value of 0.022g/kWh is?

This research study was focused on the development of an engine for on-road heavy-duty applications. The Euro VI emission regulation for such vehicles limits soot emissions to less than 0.01 g/kWh. Current soot limits for EU off-highway applications is 0.015 g/kWh, as can be seen in Stage V emission standards for non-road engines.

6) In the conclusions, in addition to summarising the actions taken and results, please highlight the novelty of this work.

The novelty of this work has been highlighted in the conclusions.

Reviewer #2

There are a few suggestions for the authors to consider.

1) To include how the '15% EGR' on page 24 was determined.

As mentioned in the Methodology, the in-cylinder air flow mass can be decreased noticeable in the combined use of Miller cycle and EGR. This will results in poor combustion instability and excessive smoke. Therefore, a moderate EGR rate of 15% was used for all cases in order to avoid the abovementioned issues as well as to achieve a fair comparison for all strategies investigated with EGR.

2) When reading the post injection strategy, the absolute value of the post injection quantity is of course important. However, the readers may like to know how much in percentage of the overall injection quantity it is.

Thanks very much for your kind suggestions. The percentage of the post injection quantity to the overall injection quantity has been added in Section 4.3.1.

3) The reference No. 53 and 55 were repeated.

Thanks. It has been corrected accordingly.